Properties of OB associations in M31

Haiman, Z.; Magnier, E.A.; Battinelli, P.; van Paradijs, J.A.; Hasinger, G.; Jain, A.; Pietsch, W.; Trumper, J.E.

Publication date
1994

Published in
Astronomy & Astrophysics

Astron. Astrophys. 290, 371–383 (1994)

ASTRONOMY AND ASTROPHYSICS

Properties of M 31 OB associations

Zoltán Haiman[1,2], Eugene A. Magnier[1,3,4], Paolo Battinelli[5], Walter H.G. Lewin[1], Jan van Paradijs[3,4], Günther Hasinger[6], Wolfgang Pietsch[6], Rodrigo Supper[6], and Joachim Trümper[6]

[1] Massachusetts Institute of Technology, Room 37-624, Cambridge, MA 02139, USA
[2] Harvard University, 60 Garden St., Cambridge, MA 02138, USA
[3] Astronomical Institute "Anton Pannekoek", Kruislaan 403, NL-1098 SJ Amsterdam, The Netherlands
[4] Center for High Energy Astrophysics, Kruislaan 403, NL-1098 SJ Amsterdam, The Netherlands
[5] Osservatorio Astronomico di Roma, Viale del Parco Mellini 84, I-00136 Roma, Italy
[6] Max-Planck-Institut für Extraterrestriche Physik, D-85748 Garching bei München, Germany

Received 12 January 1994 / Accepted 30 April 1994

Abstract. Magnier et al. (1993) recently identified 174 OB associations in M 31 using the PLC method (Battinelli 1991) with the Magnier et al. (1992) catalogue. The objectivity of the PLC method combined with the depth and accuracy of the Magnier et al. *BVRI* CCD data make these identifications suitable for photometric studies. We have studied the following properties of the 11 richest associations, 9 groups of associations, the eastern and western arms of M 31, and the entire sample of associations: the extinction E_{B-V}, the slope of the differential luminosity function (dLF) in B and V, and the slope of the initial mass function (IMF). The data are not of sufficient quality to determine the ages of associations more accurately than to show that they are younger than a few 10^7 years old.

The extinction ranges between 0.20 and 0.41 magnitudes ($\pm$0.05 mag); the western arm is significantly more reddened than the eastern arm. We have also found evidence of a difference between the young stellar populations of the eastern and western arms. The difference is most pronounced in the slopes of the B band dLF of the two arms (east: 0.46 ± 0.02, west: 0.79 ± 0.04, Δ: 0.33 ± 0.045). There is also a marginal difference seen in both the slope of the V band dLF (east: 0.48 ± 0.04, west: 0.64 ± 0.05, Δ: 0.16 ± 0.064) and the slope of the IMF (east: -2.09 ± 0.30, west: -3.02 ± 0.33, Δ: 0.93 ± 0.45). The combined weight of these three pieces of evidence suggests a real difference between the stellar populations of the two arms. It is possible that the difference is not physical, but an observational effect due to, e.g., the different reddening, varying photometric scatter between the two arms or different resolution of the images.

Key words: galaxies: M 31, photometry, star clusters, stellar content

Send offprint requests to: Eugene A. Magnier

1. Introduction

OB associations are collections of recently formed stars inside a volume $\sim 10^6$ pc^3, which can be distinguished from the background of field stars by the clustering of the bright, young O and B stars. The concentration is in general too low for them to be gravitationally bound systems. This fact, together with the fast evolution of massive stars, makes OB associations short-lived transient objects, which are therefore observed close to their birthplaces. For this reason, OB associations are natural tracers of star-forming regions, and they provide information about the formation and evolution of massive stars.

From only the spatial distribution and sizes of OB associations, one can draw an approximate map of star-forming regions, and determine the scales on which star formation is taking place. The stellar content of individual Milky Way associations, has been studied extensively (see Garmany 1991 and references therein). There are inherent difficulties in studying OB associations in our Galaxy – the poorly known distances and the high level of extinction in the Galactic plane – which make the study of OB associations in other galaxies appealing. By examining the stellar content of individual OB associations in other galaxies one can compare some fundamental properties of star formation between galaxies.

In this paper, we study the following properties of the OB associations identified by Magnier et al. (1993 – hereafter MB93) in M 31, the Andromeda Galaxy (see Fig. 1): 1) the color-magnitude diagrams, 2) the extinction, 3) the luminosity function, and 4) the initial mass function. We have only been able to determine these properties for the 11 largest and richest associations. In order to improve the statistics, we have also studied the same properties for groups of the associations. We have defined 9 groups of association, which are also shown as large circles in Fig. 1. We also determine the above properties for the entire eastern and western spiral arms of M 31 (labeled in Fig. 1).

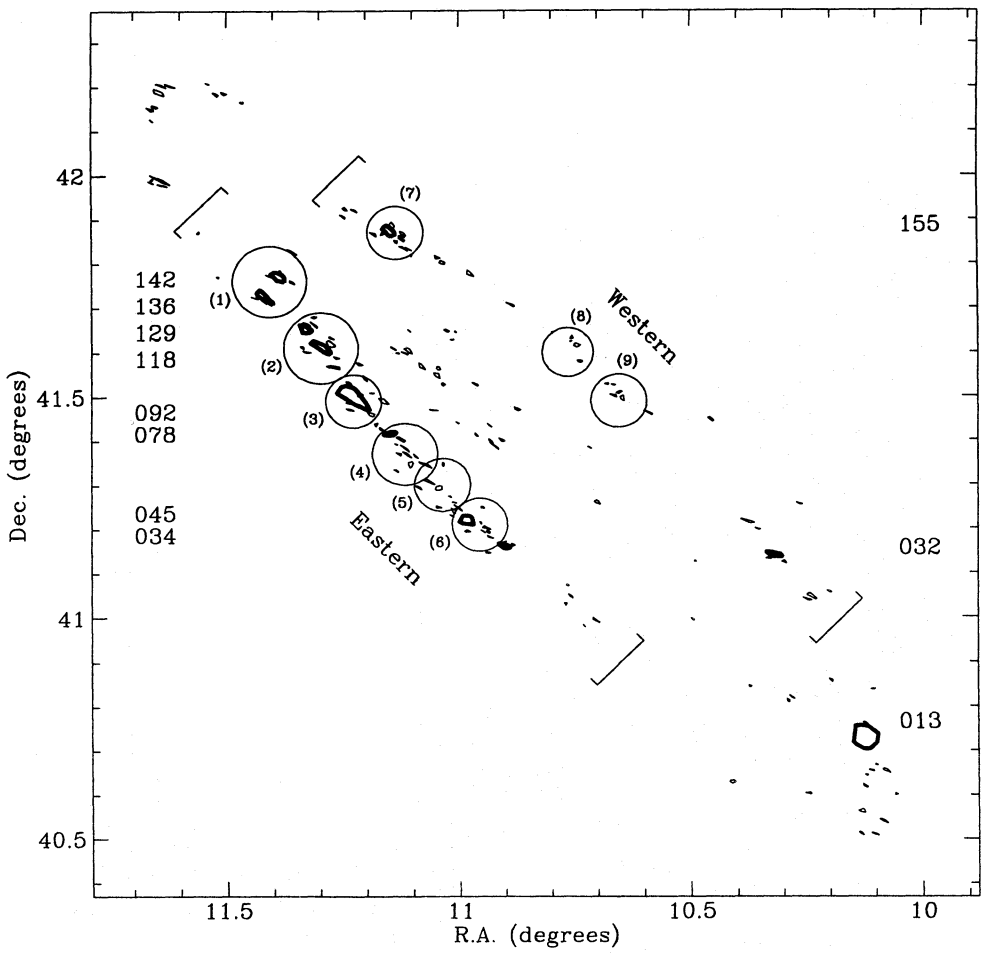

Fig. 1. The figure shows the contours of all 174 OB associations identified in M 31 by MB93. The 11 richest associations are indicated with thick lines, and marked by their numbers from Table 1 in MB93. The 9 groups are circled and numbered (see text). Axes are labeled in J2000.0 coordinates

2. The dataset

The data used for this study consist of photometric *BVRI* CCD observations of the disk regions of M 31 performed at the 1.3m McGraw–Hill telescope of the Michigan – Dartmouth – MIT (MDM) observatory during the autumns of 1990 and 1991. The observations and analysis of the 1990 data are described in detail by Magnier et al. (1992); the incorporation of data taken in 1991 and a description of the final catalogue are presented by Haiman et al. (1993). MB93 used a subset of stars from this dataset with the B and V magnitudes of O and B stars in M 31 and an objective criterion, the Path Linkage Criterion (PLC) of Battinelli (1991) to identify associations. They identified 174 OB associations, which are listed in their Table 1.

Previous studies which have identified OB associations in M 31 have had two major problems. First, the identifications were done through visual inspection of photographic plates (Efremov et al. 1987 – hereafter EIN; van den Bergh 1964 – hereafter vdB). Differences between the resolution and depth of the plates has led to disagreements among the various studies (see Hodge 1987). Also, the visual selection of the blue stars in these studies made the spectral classification rather subjective.

The second problem is the subjectivity of the definition of the individual associations. The older studies (EIN and vdB) used a visual inspection to identify the outlines of the associations. This leads to subjectivity which is particularly dependent on the different resolution of the plates used. Partly due to the use of lower resolution plates, vdB identified as "associations" significantly larger (factor of ~6) structures than those identified by EIN. There is also disagreement in the definition of the name "association". The term "complex" was used by EIN to describe essentially the same structures as those identified by vdB as "associations", while EIN used the term "association" to describe the more compact clumps of bright stars. For a further discussion of these problems, see MB93 and the footnote in Hodge (1987). MB93 avoided these problems by using the objective PLC method with a sample of stars chosen rigorously by their CCD photometry.

In this study, we have used all stars in the photometric catalogue (Magnier et al. 1992; Haiman et al. 1993) to measure properties of the OB associations. In order to select from the catalogue those stars which are in the associations, but which were not used to identify the associations (i.e., those stars which did not satisfy the B and V criteria), we drew the convex contour of each association and accepted all stars which fell within the contour. In this way, the boundary of each association was determined by the OB stars in the MB93 subset, but its stellar content was then taken from the complete catalogue. This method has the advantages that (1) it is fully objective, and (2) it preserves the shape of the associations.

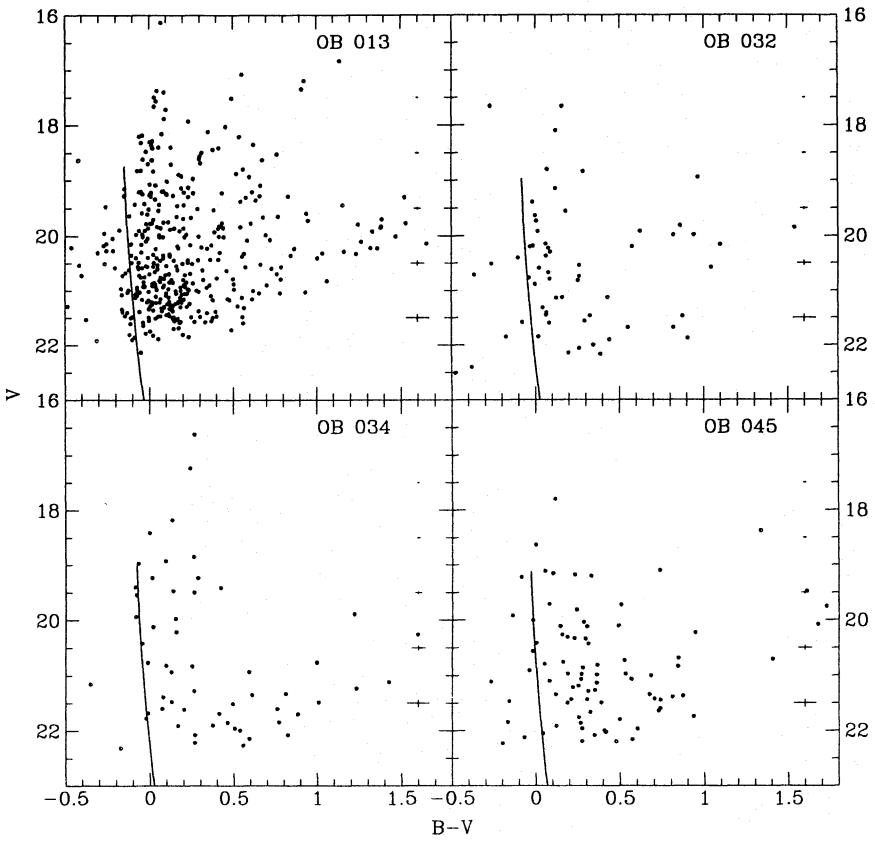

Fig. 2. Observed V, $B-V$ CMDs of OB 013, OB 032, OB 034, and OB 045. On each of the four plots, the main sequence (from SSM92) is reddened with the E_{B-V} value from Table 1. The five crosses at the right of each panel show the typical photometric errors at various magnitudes

The total number of stars in the 174 associations is 3477. A map of the spatial distribution and outlines of the associations is shown in Fig. 1. On this map, we marked the positions of the 11 largest associations, each of which contains more than 50 stars. The numbers next to these associations are the identification numbers assigned by MB93. Table 1 in MB93 gives a listing of the position, size and number of stars for each of the 174 associations. The largest association in this table, OB 013, is the most well-known association in M 31, the giant star-forming region also known as NGC 206, and also called OB 78 by Van den Bergh (1964).

3. Color-magnitude diagrams

Figures 2 – 6 present V, $B-V$ color-magnitude diagrams (CMDs) for each of the 11 richest associations and the nine groups of associations. In these plots, the solid line represents the main sequence (MS), corrected for the distance of M 31 (690 kpc – e.g., Welch et al. 1986) and the extinction measured below (Sect. 4). The MS was determined from the evolutionary tracks of Schaller et al. (1992 – hereafter SSM92), and converted from M_{bol} vs. T_{eff} into absolute V, $B-V$ values using the equations in Massey et al. (1989a). This is further described below (Sect. 6). In Fig. 7 we present the expected number of foreground stars in several portions of the CMD of OB 013. The numbers were obtained using the model of the Milky Way by Ratnatunga & Bahcall (1985), and shows rough agreement with estimates from our own data. The region with $B-V > 0.8$ and $V > 21$ is empty due to the incompleteness. It is clear from this figure that most of the detected stars are expected to be stars in M 31.

The overall morphology of these CMDs is similar in general to the morphology of previously published CMDs of M 31 associations (e.g. Hubble 1929; van den Bergh 1966; Ivanov & Kynchev 1985; Massey et al. 1986; Odewahn 1987; Hodge & Lee 1988; Berkhuijsen & Humphreys 1989; Cananzi 1992). There are some important points to be made about these CMDs. First, the main sequence is not well defined in these plots. Many recent CMDs of OB associations in the Magellanic Clouds (see, e.g., Parker et al. 1992; Massey et al. 1989a, 1989b) show well-defined main sequences, with widths of typically 0.1 mag. There are three possible explanations for the width of the MS in Figs. 2 – 6. First, the finite resolution of the images may cause blending of neighboring stellar images, resulting in inaccurate colors. Blended star images have been recognized as a problem in determining CMDs in the past for Magellanic Cloud associations (e.g., Freedman 1983). Second, differential reddening within the association may cause a widening of the MS. CMDs of certain, dusty associations in the Magellanic Clouds show widened MSs, even with high-resolution observations (private communication, Parker). Finally, associations with a range of stellar ages, or overlapping associations of different ages may also lead to a widening of the MS. Various combinations of these three effects are probably responsible for the morphology of the CMDs in Figs. 2 – 6. These effects limit the accuracy of our determinations of the various properties of the associations.

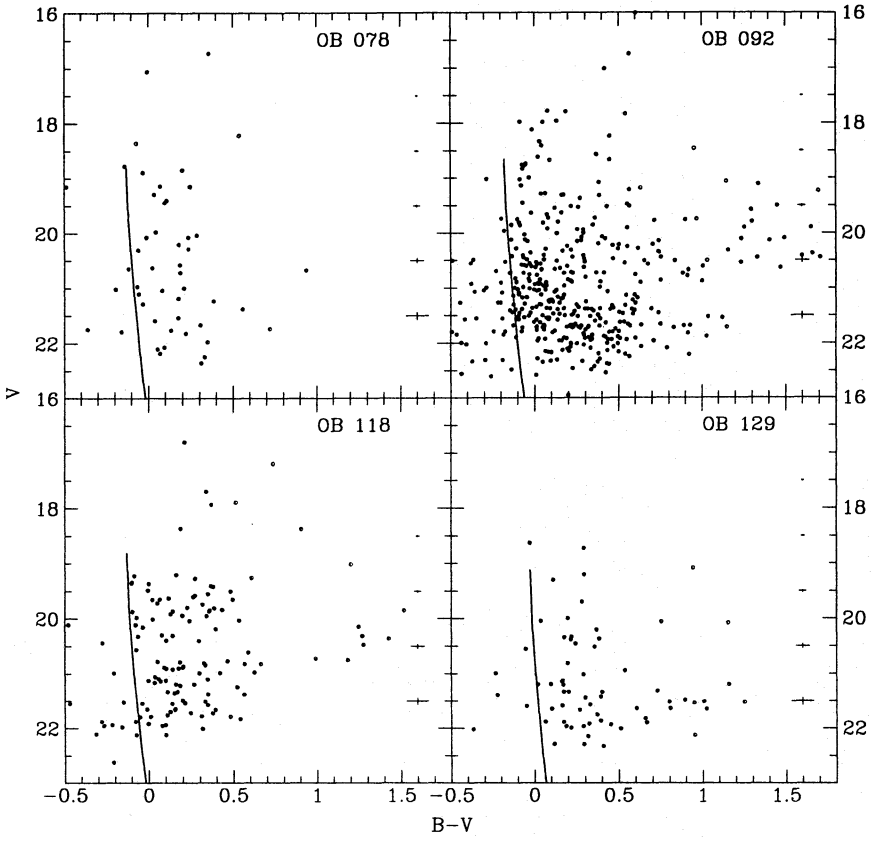

Fig. 3. Observed V, $B-V$ CMDs of OB 078, OB 092, OB 118, and OB 129. Comments are as in Fig 2

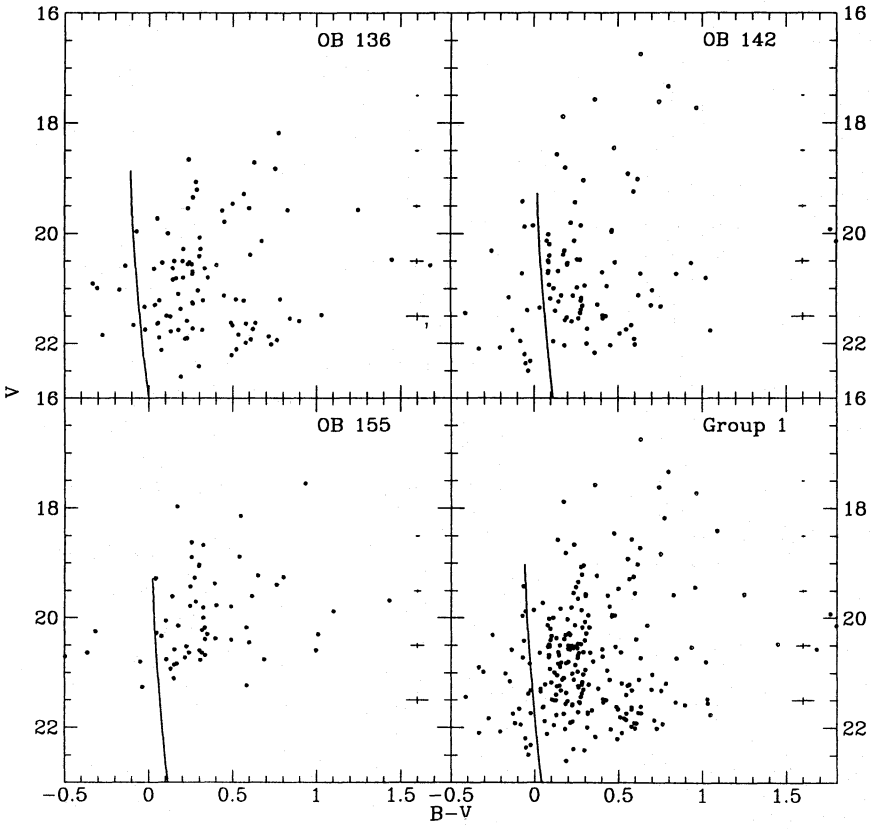

Fig. 4. Observed V, $B-V$ CMDs of OB 136, OB 142, OB 155, and group 1. Comments are as in Fig 2

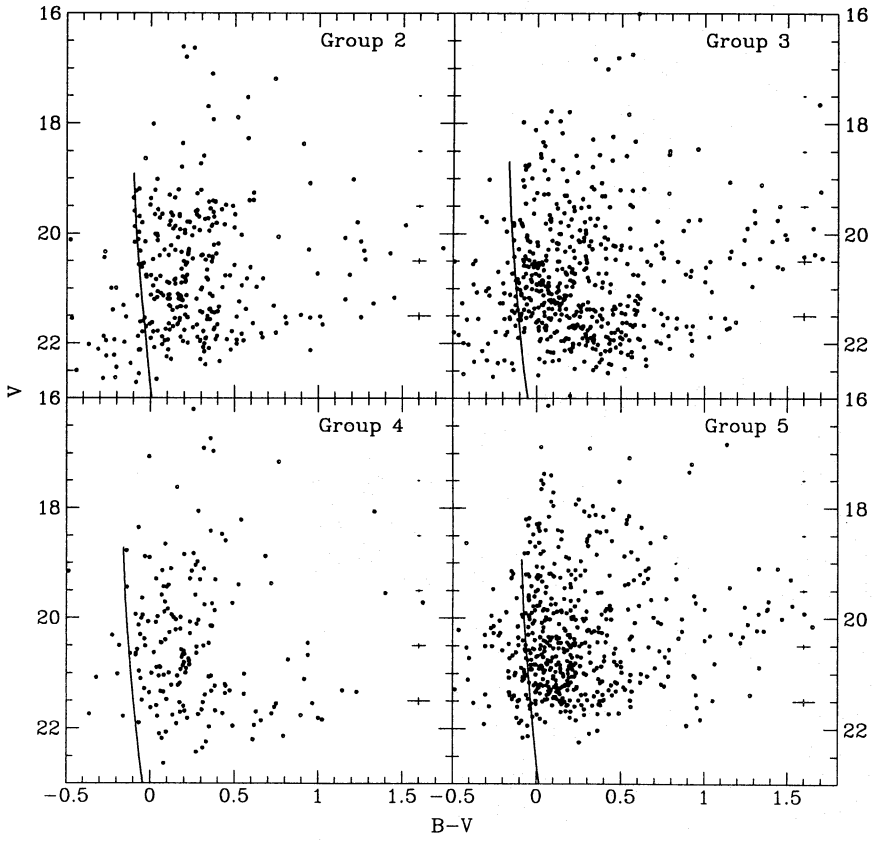

Fig. 5. Observed V, $B-V$ CMDs of groups 2, 3, 4, and 5. Comments are as in Fig 2

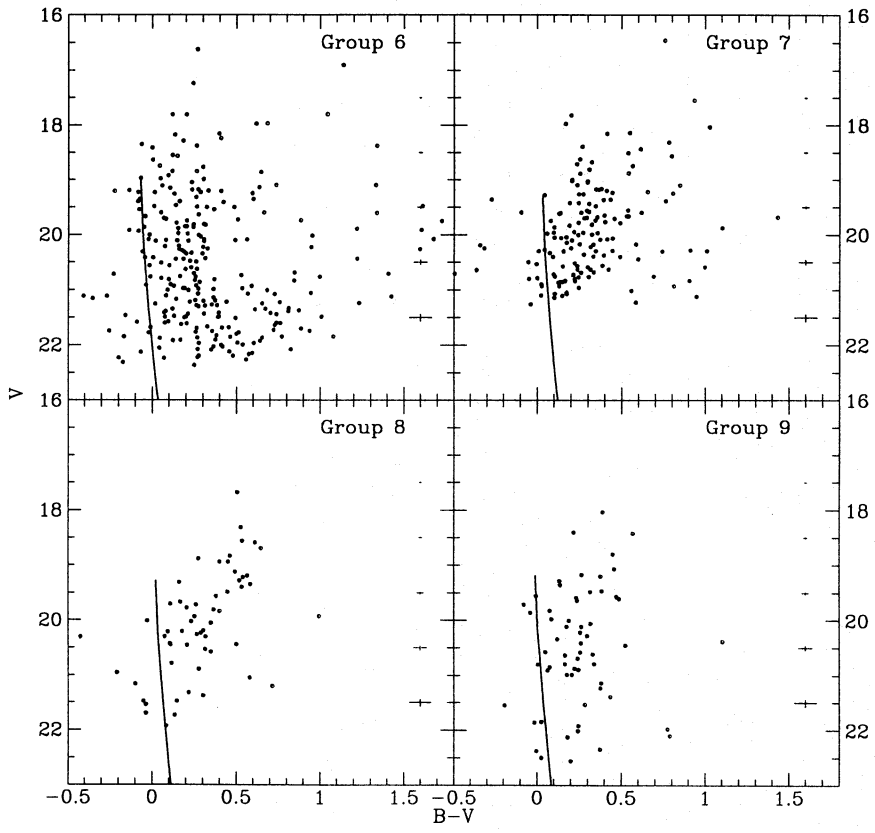

Fig. 6. Observed V, $B-V$ CMDs of groups 6, 7, 8, and 9. Comments are as in Fig 2

Table 1. Extinctions, dLF slopes (α_B, α_V), IMF slopes (α_{IMF}), and number of stars for the 11 richest associations and the 9 groups

Assoc.	E^1_{B-V}	E^2_{B-V}	α_{IMF}	σ_α	N	Region	E^2_{B-V}	α^3_B	σ_B	α^3_V	σ_V	α_{IMF}	σ_α	N
OB 013	0.25	0.23	-1.79	0.16	417	Eastern arm	0.29	0.46	0.02	0.48	0.04	-2.09	0.30	1770
OB 032	0.30	0.28			60	Group 1	0.32	0.44	0.04	0.44	0.08	-2.65	0.36	237
OB 034	0.30	0.27			60	Group 2	0.28	0.40	0.07	0.50	0.07	-2.20	0.09	319
OB 045	0.35	0.35			86	Group 3	0.21	0.54	0.06	0.52	0.09	-1.74	0.16	597
OB 078	0.25	0.24			51	Group 4	0.22	0.33	0.06	0.35	0.08	-2.28	0.28	184
OB 092	0.20	0.20	-1.56	0.21	433	Group 5	0.29	0.43	0.04	0.43	0.04	-2.51	0.19	160
OB 118	0.25	0.24	-1.68	0.22	131	Group 6	0.31	0.46	0.05	0.54	0.11	-1.86	0.18	273
OB 129	0.30	0.35			67	Western arm	0.41	0.79	0.04	0.64	0.05	-3.02	0.33	273
OB 136	0.25	0.32			95	Group 7	0.41	0.63	0.05	0.54	0.03	-2.64	0.16	154
OB 142	0.30	0.29	-1.95	0.21	100	Group 8	0.40	0.69	0.06	0.58	0.19	-2.10	0.30	58
OB 155	0.40	0.41			62	Group 9	0.37	0.59	0.16	0.66	0.26	-2.21	0.35	61

[1] Value from subjective method. (error ~0.10)
[2] Value from objective method. (error ~0.05)
[3] determined for $B - V < 0.4$

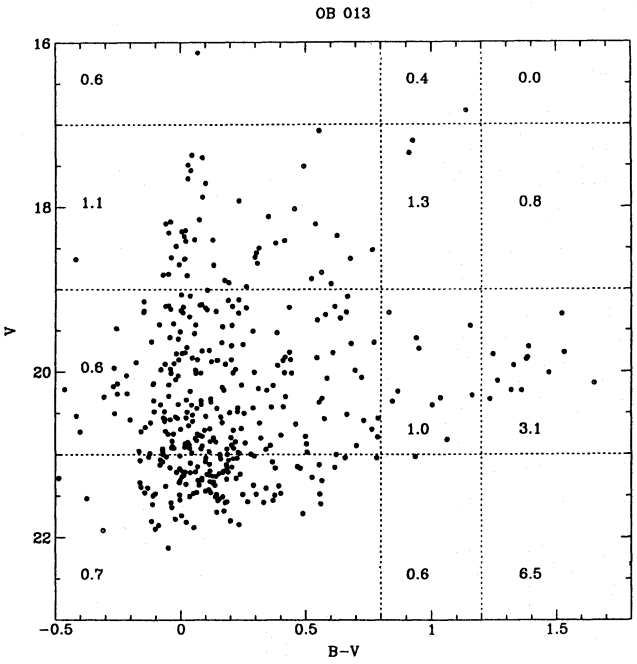

Fig. 7. Foreground contamination in the CMD of OB 013. The plot shows the observed V and $B - V$ values for OB 013. The number in each box is the expected number of foreground stars calculated from Ratnatunga & Bahcall (1985). The lack of stars within the region $V \geq 21$ and $B - V \geq 0.8$ is due to incompleteness

4. Extinction

We have determined the average extinction for the 11 richest associations, the 9 association groups, and the eastern and western spiral arms (Table 1). There are several possible ways of determining the extinction of an association using broad-band data, and we experimented with three methods. First, we attempted to employ theoretical isochrones in various color-color diagrams (i.e., $B - V, V - I$ or $B - V, V - R$), but we found that the data were not sufficiently accurate to determine either the extinction or the extinction law (as parametrized by $R_V \equiv A_V/E_{B-V}$). This is partly because in the only color-color diagrams we could construct, the reddening line and the locus of main-sequence stars are nearly parallel, with the result that there is too much degeneracy to accurately constrain E_{B-V} or R_V (see Fig. 8A).

We therefore adopted $R_V = 3.1$, which is both the Galactic value and consistent with the current best estimate for M 31 (Walterbos & Kennicutt 1988). The two methods we used to determine the extinction involved "fitting" the main sequence (MS) to the observed V, $B - V$ CMDs. Figures 8B and 8C demonstrate these two methods. Figure 8B shows the CMD for OB 013. The four tilted lines are the expected location of the MS for $E_{B-V} = 0.0$, 0.1, 0.2, and 0.3, using the adopted value of R_V. By shifting the theoretical MS in the direction (1, 3.1) on the CMD, we can determine the reddening by finding the value of E_{B-V} which provides the best "fit" to the MS. For this purpose, the theoretical MS was obtained by joining the starting points of the evolutionary tracks of SSM92, which is further described below (Sect. 6). As expected, the accuracy of this method depends on how well the MS is "defined" on the CMD of each association.

It is possible to determine E_{B-V} from the CMDs by eye. We used plots similar to Fig. 8B with several intermediate E_{B-V} values, and with various scales for the axes, to find estimates for E_{B-V} for each of the 11 richest associations (see Table 1). We call this the "subjective" determination of E_{B-V}. For OB 013, we concluded that E_{B-V} is ~0.25, with an uncertainty of ~0.1 mag, which is a typical error for this method. For the less rich associations, determining E_{B-V} in this way is more difficult.

To introduce a less subjective determination of E_{B-V}, and to double-check the values determined by eye, we adopted the following simple method to determine E_{B-V}. Starting with

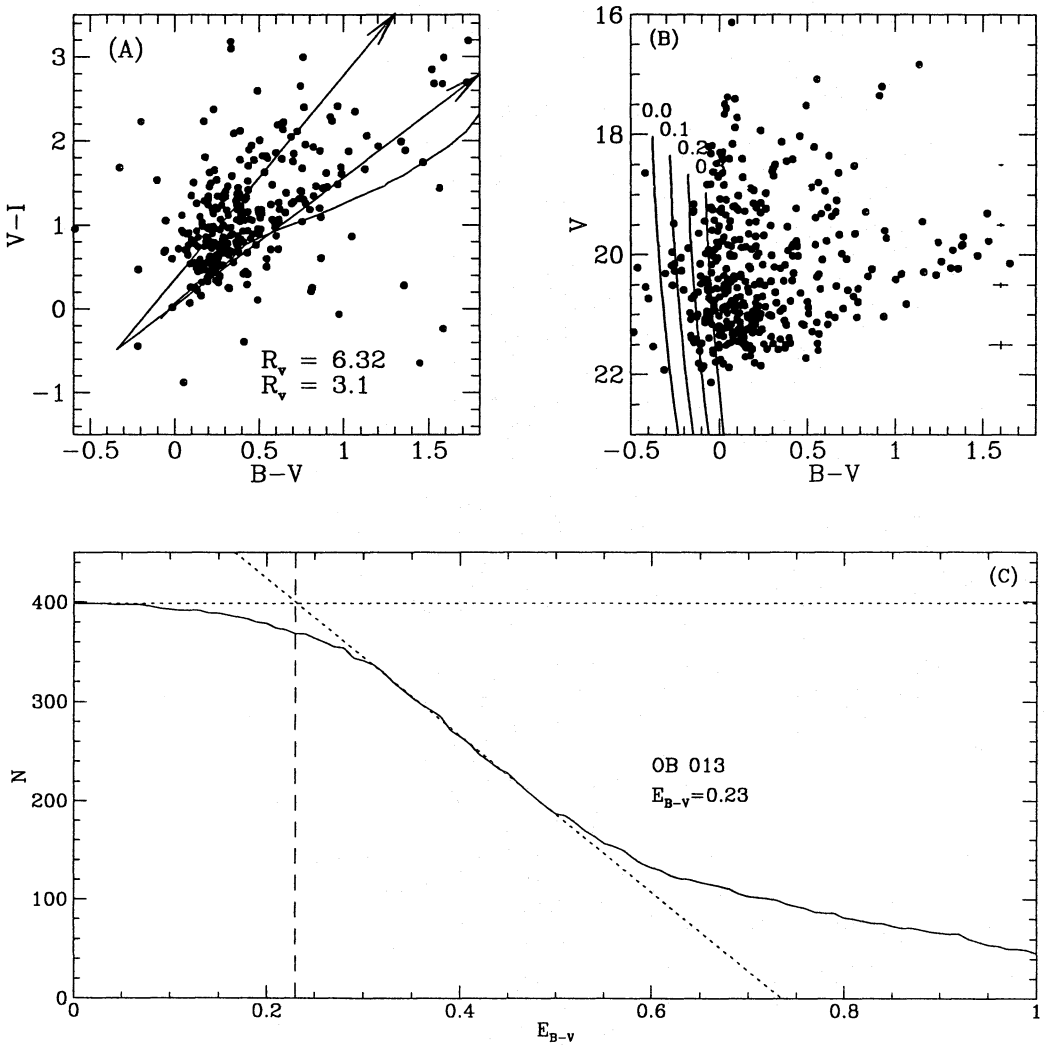

Fig. 8. a $B-V, V-I$ Color-color diagram of OB 013 showing the unreddened location of the main sequence (MS) and two example reddening vectors: R_V = 3.1 (upper arrow) and 6.3 (lower arrow). It is clear that E_{B-V} and R_V are not well determined by this diagram. **b** CMD of OB 013 showing the location of the MS for E_{B-V} = 0.0, 0.1, 0.2, and 0.3. **c** E_{B-V} vs. N_{stars}: Objective determination of the extinction to OB 013 using the CMD

E_{B-V} = 0.0, we drew the MS, and counted the number of stars redward and blueward of the MS. We performed the same counting for several positions of the MS, corresponding to the range $0.0 < E_{B-V} < 1.0$. Finally, we plotted the number of stars to the right of the MS as a function of E_{B-V}. Figure 8C shows the results for OB 013. We determined E_{B-V} as the intersection of a horizontal line representing the number of stars when all the stars are to the right of the MS (for low E_{B-V}) and a line-fit in the region of E_{B-V} where stars start to fall to the left of the main sequence. We call this the "objective" determination of E_{B-V}. With this method, E_{B-V} was found to be 0.23 ± 0.02 in OB 013, in very good agreement with the subjectively determined value, and also with the value of 0.27 ± 0.03 found by Odewahn (1987). Table 1 shows the extinction of the 11 richest associations as determined by both objective and subjective methods. The anomalously high extinction in OB 155, $E_{B-V} \sim 0.41$ is also confirmed by both methods.

One might suspect that these methods will result in systematically higher E_{B-V} values for associations with fewer stars. To account for this possibility, we determined the extinction for the 9 groups of associations and the eastern and western spiral arms (see Fig. 1). It is clear that the extinction of the western arm is significantly higher than that of the eastern arm, and this does not appear to be due to the different total number of stars. It has been noted previously (e.g., Hodge & Kennicutt 1982) that the western dust lane is deeper and more pronounced than the eastern one. It has been suggested that this difference is due to the inclination of M 31: the eastern arm is on the far side of the bulge, and is muted by the contaminating presence of bulge stars. However, our result suggests a real difference since the bulge stars should not significantly affect our measurement of the association E_{B-V}.

It is interesting to note that there are about half as many OB associations along the western spiral arm as along the east-

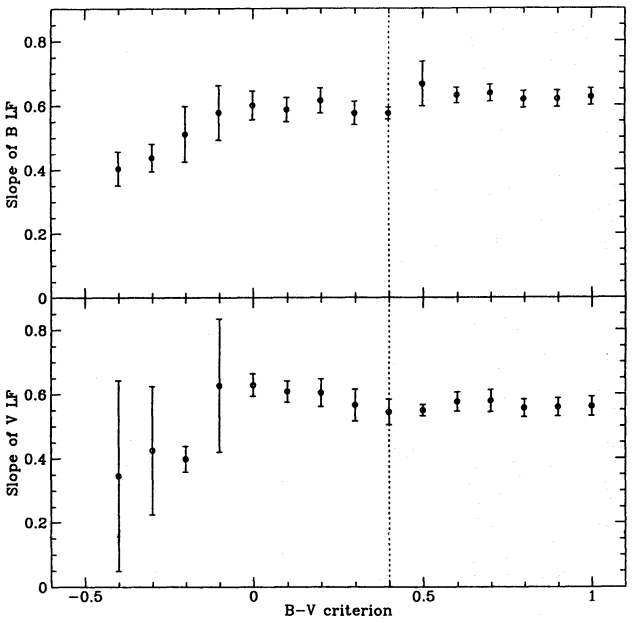

Fig. 9. Variation of the slope of the luminosity function with $B-V$ color criterion. In each case the data included in the determination of the dLF are those stars which are bluer than the given color cutoff. Foreground contamination would flatten the slopes above $E_{B-V}\sim 0.4$ (dotted line)

ern arm. In principle, higher extinction within the western arm could be responsible for this imbalance. However, this seems unlikely since the sample of stars used by MB93 to identify the associations included stars which were reddened by E_{B-V} up to 1.0 mag. Walterbos & Kennicutt (1988) also noted this difference in the number of associations and concluded from the uniformity of "reddening-free" images that the difference was not due to dust obscuration. Other than the difference between the spiral arms, we detected no systematic variation of E_{B-V}. The extinction seems to vary randomly from one association to the other, and from group to group.

5. The differential luminosity function

The differential luminosity function $\phi(M)$ (dLF) expresses the number of stars per unit magnitude interval, as a function of the absolute magnitude. The total number of stars $N(M)$ with absolute magnitude between M and $M+dM$ is given by $\phi(M)dM$. An approximation of the dLF can be obtained from photometric data as $\Phi(M)\sim N(M, M+\Delta M)/\Delta M$, where the binsize ΔM is finite ($\sim$ 0.7 mag in our case).

The dLF is an important quantity because differences in stellar populations should be reflected in the dLF. The dLF is often assumed to be a power law function, in which case the "slope of the dLF" $\alpha \equiv \frac{d\log\phi(M)}{dM}$ is a constant. An interesting question is whether this constant varies locally on small scales, but has a universal value when averaged over sufficiently large scales. For instance, Berkhuijsen (1983) determined the dLF for several associations in M33, and claimed variations of about a factor of 2 in the slopes, yet Freedman (1985) claimed the dLF slope did not vary significantly from galaxy to galaxy. In constructing the dLFs directly from the B and V data, two caveats are the small number of stars in individual associations, and contamination by non-member stars, either in the foreground or evolved stars in M 31.

We account for the small number of stars in the associations by using the groups of associations described above (Sect. 1). Figure 7 suggests that the foreground contamination is a negligible problem. To double-check this, we examined the slope of the combined dLF of all associations in M 31 for different values of a $B-V$ criterion; that is, we only include stars which are bluer than a given color cutoff. If foreground contamination had a significant effect, it would show up as a systematic flattening of the dLF for redder values of the cutoff. Figure 9 shows the slope of the dLF in B and V as a function of the cutoff. Below, we discuss the method used to determine the slope. In these plots, stars from all of the associations were included to determine the dLF. The slopes do not vary systematically for higher values of the cutoff. The systematic flattening of the slope for low values of the cutoff is due to the fact that the sample becomes too small (Freedman 1985). We conclude that the contamination by foreground stars is small enough to be considered negligible. We do not attempt to remove evolved non-association members using a stricter $B-V$ cutoff, as has been done by other authors (e.g., Freedman 1985; Berkhuijsen & Humphreys 1989). We make this choice for two reasons: 1) our samples are chosen in relatively compact regions surrounding the OB associations; thus the bulk of the general M 31 disk stars should be excluded. 2) Evidence from recent CMDs of LMC associations suggests that the width of the MS (see Figs. 3 – 6) is not due to evolved stars but instead to the effects of blending and differential reddening (see below). Without the *a priori* knowledge that the stars on the right side of the MS are evolved, we choose to included them in our samples. The fact that our results are consistent with those of Berkhuijsen & Humphreys (1989, see below) lends support to these arguments.

Table 1 lists the measured slopes of the B and V dLFs for the nine groups and the eastern and western spiral arms. Figures 10 and 11 show the differential luminosity functions determined for the nine groups, while Fig. 12 shows the B and V dLFs for the eastern and western spiral arms. These figures also show the linear fits to the dLFs, excluding those bins which are incomplete. Complete bins ($16.5 < B < 21$; $16.5 < V < 20$) are represented by filled circles, while the incomplete bins by open circles. We note that the B dLF is significantly steeper for the western arm than for the eastern arm (east: 0.46 ± 0.02, west: 0.79 ± 0.04, Δ: 0.33 ± 0.045). There is also a marginal difference seen in the slope of the V dLF (east: 0.48 ± 0.04, west: 0.64 ± 0.05, Δ: 0.16 ± 0.064). This difference confirms the difference noted by Berkhuijsen & Humphreys (1989) for the dLFs measured for their entire sample of stars for both arms.

For comparison with previous studies, we determined the dLF within the largest association, OB 013 (NGC 206). The results are shown in Fig. 13. We found the slope in B to be 0.47 ± 0.06, which is identical to the value found by Odewahn

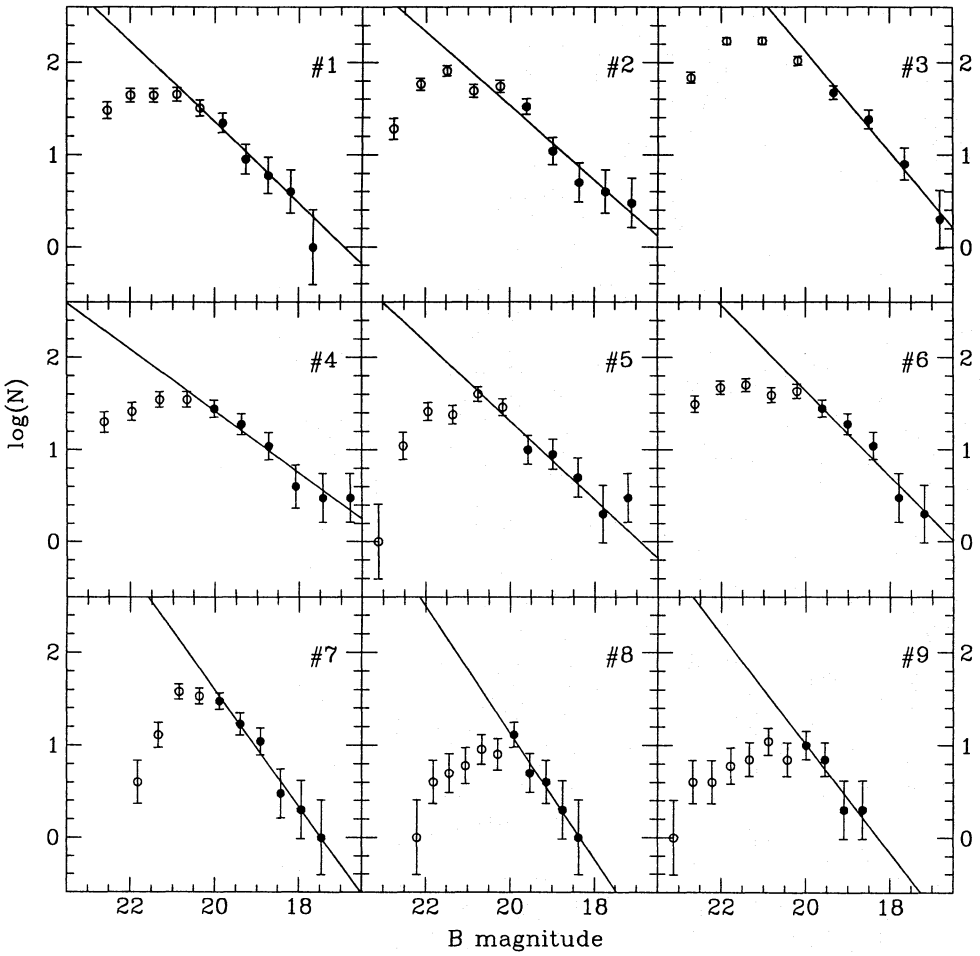

Fig. 10. Weighted least-squares fits to determine the slope of the B differential luminosity function within the nine groups of OB associations. As a conservative estimate of completeness, the bins with mag $\geq$ 20.6 were ignored in the linear fits (empty circles). Groups 1 – 6 are on the eastern arm, groups 7 – 9 are on the western arm, as in Fig. 1

(1987), (0.47$\pm$0.06). The slopes of the overall B and V dLF for all OB associations in M 31 are 0.61 $\pm$ 0.03 and 0.62 $\pm$ 0.05. These results are consistent with the conclusion of Freedman (1985), that the dLF of upper main-sequence stars in nearby galaxies does not vary significantly from one galaxy to the other. For instance, the values for M33 are 0.65$\pm$0.03 and 0.67$\pm$0.05.

6. The initial mass function

The initial mass function (IMF) can be constructed from the CMDs with the help of theoretical evolutionary tracks for stars of a range of masses: the number of stars in a given mass interval can be obtained by simply counting the number of stars between the corresponding pair of evolutionary tracks. This is demonstrated for OB 013 in Fig. 14, which uses evolutionary tracks from SSM92. With this technique, we obtain the present-day, or "observed" mass function (PDMF). In general, the IMF is obtained from the PDMF by making corrections for the stars which have died throughout the history of the system. In order to make these corrections, one must know the stellar birthrate history of the system. In past photometric work on OB associations, one of two approximations about the birthrate have been made.

The simpler of the two approximations is that all stars within one association were born at the same time. This assumption is quite justified for associations such as LH 9 or LH 10 in the LMC (Parker et al. 1992): the MS in both of these associations is very tight and there is no evidence of differential evolution. The same assumption has also been made about OB associations in M 31 (Massey et al. 1986). The other approximation that has been made is to assume that the birthrate has been constant since some initial time, i.e., since the formation of the least massive stars (Odewahn 1987). Because most of our associations contain only a small number of stars, in this paper we adopt the simplest assumption, i.e., we consider all the stars within one association to have been formed at the same time. With this assumption, the IMF is equivalent to the PDMF for stars of masses which have not yet evolved off the CMD.

SSM92 published several sets of theoretical evolutionary tracks. The determined IMF could, in principle, depend on which of these sets of tracks are used. Garmany et al. (1982) discussed the consequences of using three different types of

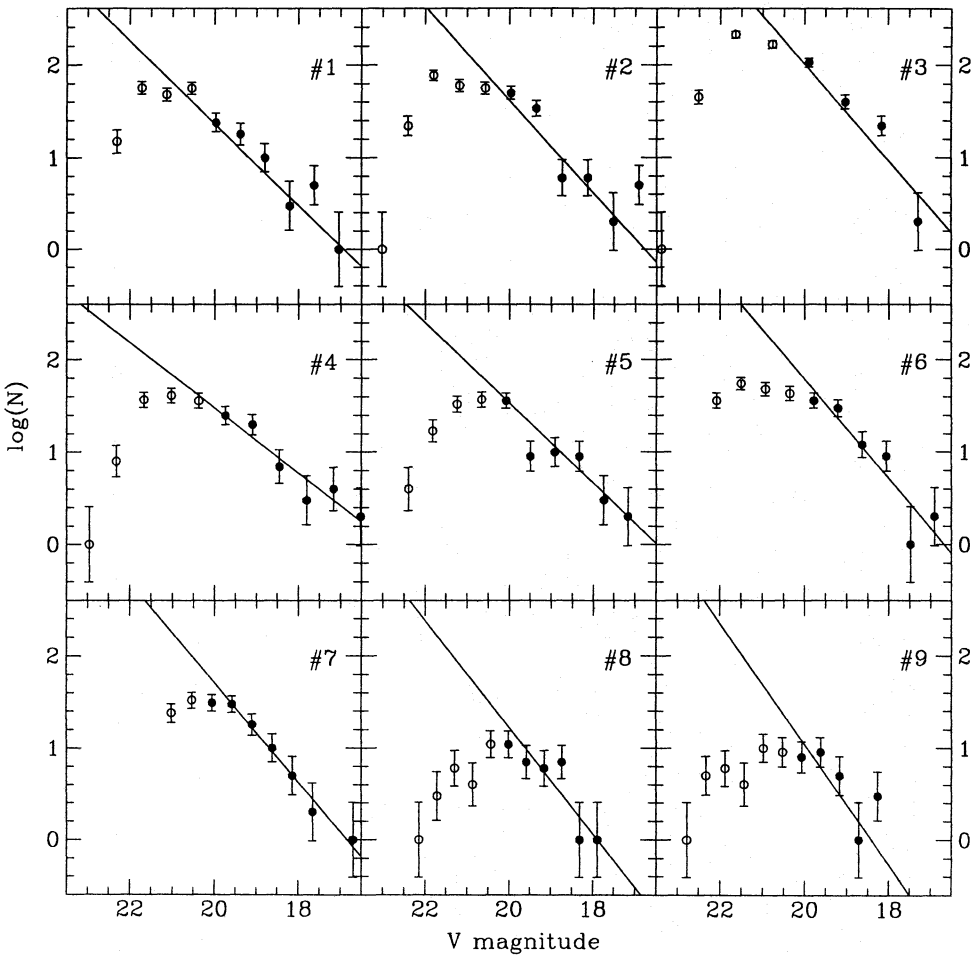

Fig. 11. Weighted least-squares fits to determine the slope of the V differential luminosity function within the nine groups of OB associations (see Fig. 10)

tracks (no mass loss, mass loss, and convective overshooting) to determine the mass function. Their results showed that the effects were rather minor, i.e., the change in the slope of the IMF was insignificant. For our IMF determination we have adopted the recent solar metallicity (Z=0.02) evolutionary tracks with mass loss published by SSM92. We smoothed each track into a monotonic curve by omitting the details of the evolution: this did not change the IMF significantly, but it enabled the automatic counting of stars between tracks.

In order to exclude incomplete mass intervals when determining the slope of the IMF, we converted the V completeness limits into mass completeness limits with the help of the mass tracks and the CMD. We also excluded the highest mass bins, because the statistics of the very small number of stars in those bins are unreliable. We found that the interval $0.9 \lesssim \log(M/\mathrm{M}_\odot) \lesssim 1.5$ is most suitable to determine the IMF.

We used the V, $B-V$ CMDs to find the IMF for the 4 richest OB associations (Fig. 15), the nine groups of associations (Fig. 16), and the eastern and western spiral arms (Fig. 17). As with the dLFs, we have fit the IMFs with a power law and determined the slope of the IMFs. The resulting slopes are found in Table 1. We have also determined the IMF slope for the entire sample of OB association stars (Table 2). We show in Fig. 15 the two IMFs determined for OB 142 when all mass bins were included, and when only reliable mass bins (solid dots) were included. The slope derived was quite different in the two cases, showing that the derived slope of the IMF is dependent on the completeness limits, and the statistics of the highest mass bins. By grouping associations together, our initial assumption that the stars in the sample were born roughly at the same time is weakened. An age difference between two associations has an effect on the high-mass end of the IMF, because the most massive stars might be present in the younger association, while they might have evolved away from the CMD of the older association. However, in determining the slope of the IMF, we have excluded the high-mass end, where stars may have evolved away. Therefore, as long as the age difference between the two associations is small, we can expect that the slope of the IMF we derive will not be affected significantly.

We note that the IMF slope is marginally different for the western and eastern arms (east: -2.09 ± 0.30, west: -3.02 ± 0.33, Δ: 0.93 ± 0.45). By itself, this is not a strong effect (2.1σ), but the combined weight of the three pieces of evidence – B dLF slope, V dLF slope, IMF slope – suggests a real difference

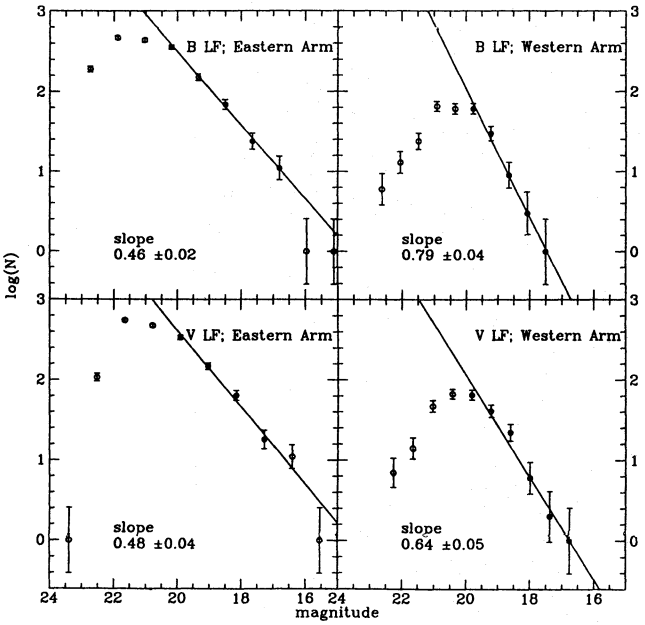

Fig. 12. B and V differential luminosity functions within the eastern and the western spiral arms. Empty circles represent incomplete magnitude bins, and were not used in the linear fits. Both dLFs are steeper in the western spiral arm

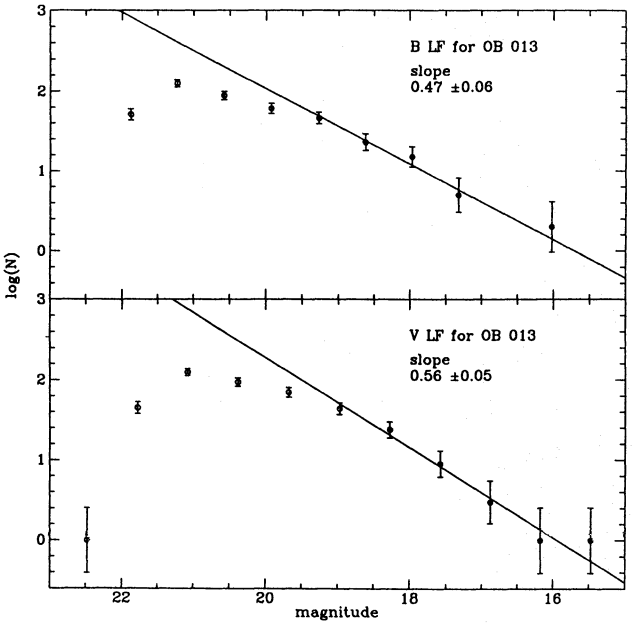

Fig. 13. B and V differential luminosity functions within OB 013. The slope in B (0.47 ± 0.06) agrees with the result by Odewahn (1987)

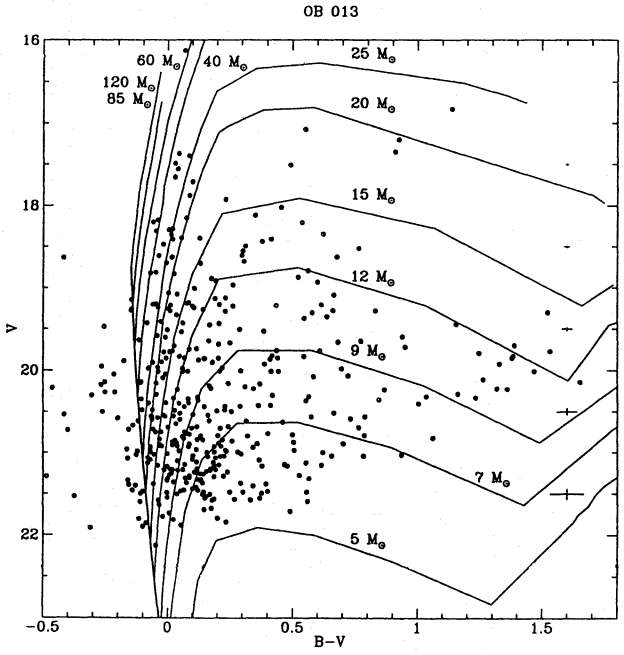

Fig. 14. Observed CMD of OB 013 showing mass tracks of SSM92. The crosses show the typical photometric errors at various magnitudes. The mass tracks are reddened with $E_{B-V} = 0.23$

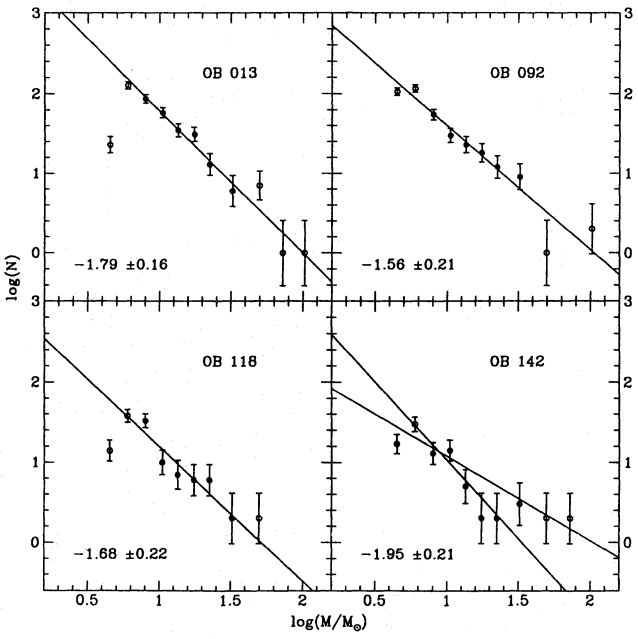

Fig. 15. Initial mass functions within the 4 largest associations, with derived slopes. The empty circles were excluded from the weighted linear fits (see text). The number of stars in OB 013, OB 092, OB 118, and OB 142 is 433, 417, 133, and 100, respectively. The slope for OB 142 when including all points for the fit is -2.2 ± 0.46

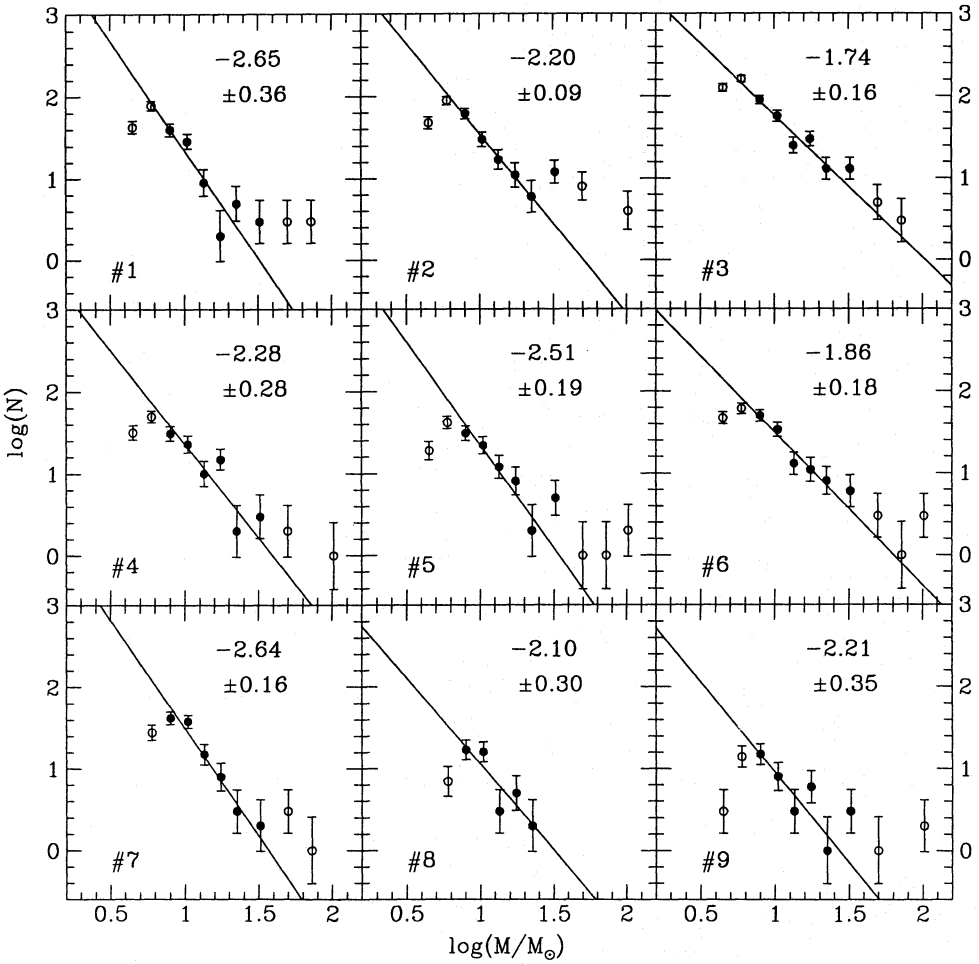

Fig. 16. Initial mass functions within 9 groups of associations. The derived slopes and formal weighted least-squares fit errors are shown. Groups 1-6 are in the eastern arm, groups 7-9 are in the western arm, as in Fig. 6

Table 2. Recent IMF slope measurements in Local Group galaxies

Galaxy	α	σ_α	Reference
Milky Way	-2.41	-	Humphreys et al. (1984)
LMC	-2.29	-	Humphreys et al. (1984)
LMC (LH117)	-1.80	0.10	Massey et al. (1989a)
LMC (LH118)	-1.80	0.10	Massey et al. (1989a)
SMC	-2.14	-	Humphreys et al. (1984)
SMC (LH 9)	-1.60	0.10	Parker et al. (1992)
SMC (LH 10)	-1.10	0.10	Parker et al. (1992)
SMC (NGC 346)	-1.90	0.30	Massey et al. (1989b)
M33	-2.20	0.50	Odewahn 1987
M 31 (OB 013)	-2.00	0.25	Odewahn 1987
M 31 (OB 013)	-1.79	0.16	this paper
M 31 (OB 092)	-1.56	0.21	this paper
M 31 (OB 118)	-1.68	0.22	this paper
M 31 (OB 142)	-1.95	0.21	this paper
M 31 (E. arm)	-2.09	0.30	this paper
M 31 (W. arm)	-3.02	0.33	this paper
M 31 (Overall)	-2.06	0.23	this paper

between the stellar populations of the two arms. Note that, while the B and V band dLFs contain information similar to the IMF, the three are distinct measurements due to the application of the color information in the determination of the IMF. Finally, in Table 2, we list recent measurements of the IMF in various Local Group galaxies for comparison with our own measurements.

7. Conclusion

We have examined the stellar content of the 174 OB associations recently identified in the field of M 31 by MB92. From color-magnitude diagrams of each association, we have determined the extinction E_{B-V}, the differential luminosity function, and the initial mass function. We have determined most of these quantities for the 11 richest associations, 9 groups of associations, the eastern and western spiral arms, and the entire sample of OB associations.

The extinction was found to vary between 0.20 and 0.41 magnitudes (±0.05 mag). The extinction was found to be significantly higher for the western arm than for the eastern arm. We have also found evidence of a difference between the young stellar populations of the eastern and western arms. The distinc-

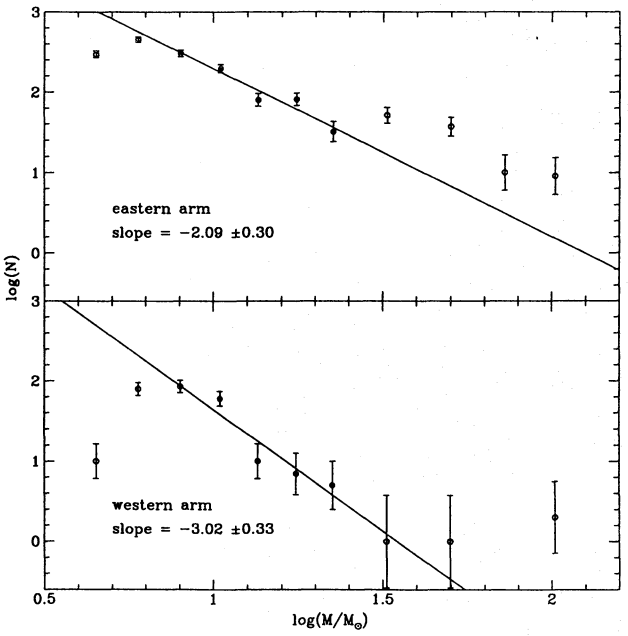

Fig. 17. Initial mass functions with all stars from the eastern / western spiral arms. The derived slopes and formal weighted least-squares fit errors are shown. The IMF is steeper along the western spiral arm

tion is evident in a pronounced difference in the slope of the B dLF of the two arms (east: 0.46 ± 0.02, west: 0.79 ± 0.04, Δ: 0.33 ± 0.045). There is also a marginal difference seen in both the slope of the V dLF (east: 0.48 ± 0.04, west: 0.64 ± 0.05, Δ: 0.16 ± 0.064) and the slope of the IMF (east: -2.09 ± 0.30, west: -3.02 ± 0.33, Δ: 0.93 ± 0.45). The combined weight of these three pieces of evidence suggests a difference between the observed properties of the stellar populations of the two arms. It is possible that the difference is not physical, but an observational effect due to, e.g., the different reddening, varying photometric scatter between the two arms or different resolution of the images.

As noted in Sect. 3, the study of OB association properties in M 31 is hampered by three effects: 1) blended star images, 2) differential internal reddening, and 3) overlapping associations in the images. It is difficult to overcome all three problems, but much progress can eventually be made by increasing the resolution and depth of the images used, and by using UV and far-UV data to determine the extinction of the stars. Spectral stellar classification is also desired (see, e.g., Parker et al. 1992), though rather difficult for these faint stars. Future studies of the differences between the spiral arms are encouraged to determine if the variations in the dLFs and IMFs are due to the stellar populations, or if they are the result of extinction or observational limitations.

Acknowledgements. Observations discussed in this paper were performed at the Michigan – Dartmouth – MIT (MDM) Observatory. We would like to thank the MDM TAC for the generous amounts of telescope time devoted to this project. We are also grateful for A. Maeder for providing us with the evolutionary tracks in a convenient electronic format. We greatly appreciate the helpful comments provided by Paul Hodge, Myung Gyoon Lee, Joel Parker, Kelly M. Torikai, and Sydney van den Bergh. WHGL is supported by the United States National Aeronautics and Space Administration under grants NAG5-1441 and NAGW-3234. JvP acknowledges support from NATO through grant RG 331/88. EAM acknowledges support by the Netherlands Foundation for Research in Astronomy (ASTRON) with financial aid from the Netherlands Organization for Scientific Research (NWO) under contract number 782-376-011.

References

Battinelli P. 1991, A&A 244, 69
Berkhuijsen E.M. 1983, A&A 127, 395
Berkhuijsen E.M. & Humphreys R.M. 1989, A&A 214, 68
Cananzi 1992, A&A 259, 17
Efremov Yu.N., Ivanov G.R., Nikolov N.S. 1987, Ap&SS 135, 119 [EIN]
Freedman W. 1983, in IAU Colloquium 76, *The Nearby Stars and the Stellar Luminosity Function*, ed A. G. Davis Philip (Schenectady: L. Davis Press), p. 191
Freedman W. 1985, ApJ 299, 74
Garmany C.D. 1991, in ASP Conference Series Vol. 13, *The Formation and Evolution of Star Clusters*, ed. K. James
Garmany C.D., Conti P.S., Chiosi C. 1982 ApJ 263, 777
Haiman Z., Magnier E.A., Lewin W.H.G., et al. 1994, A&A in press
Hodge P.W. 1987, PASP 99, 173
Hodge P.W. & Kennicutt R.C. 1982, AJ 87, 264
Hodge P.W., Lee M.G. 1988, ApJ 329, 651
Hubble E.E. 1929, ApJ 69, 103
Humphreys R.M. & McElroy D.B. 1984, ApJ 284, 565
Ivanov G.R. & Kynchev P.Z. 1985, Sov. Astr. Lett. 11, 5
Magnier E.A., Battinelli P., Haiman Z., et al. 1993, A&A 278, 36 [MB93]
Magnier E.A., Lewin W.H.G., van Paradijs J., et al. 1992, A&AS 96, 379
Massey P., Armandroff T.E., Conti P.S. 1986, AJ 92, 1303
Massey P., Garmany C.D., Silkey M., Degioia-Eastwood K., 1989a, AJ 97, 107
Massey P., Parker J.W., Garmany C.D. 1989b, AJ 98, 1305
Odewahn S. 1987, AJ 92, 310
Parker J.W., Garmany C.D., Massey P., Walborn N.R., 1992, AJ 103, 1205
Ratnatunga K.U. & Bahcall J.N. 1985, ApJS 59, 63
Schaller G., Schaerer D., Meynet G., Maeder A. 1992, A&A 96, 269 [SSM92]
Van den Bergh S. 1964, ApJS 9, 65 [vdB]
Van den Bergh S. 1966, ApJ 71, 219
Walterbos R.A.M. & Kennicutt R.C. 1988, A&A 198, 61
Welch D.L., McAlary C.W., McLaren R.A., Madore B.F. 1986, ApJ 305, 583

This article was processed by the author using Springer-Verlag LaTeX A&A style file version 3.